

# Analysis of *N*-acylhomoserine lactone dynamics in continuous cultures of *Pseudomonas putida* IsoF by use of ELISA and UHPLC/qTOF-MS-derived measurements and mathematical models

Katharina Buddrus-Schiemann · Martin Rieger · Marlene Mühlbauer · Maria Vittoria Barbarossa · Christina Kuttler · Burkhard A. Hense · Michael Rothballer · Jenny Uhl · Juliano R. Fonseca · Philippe Schmitt-Kopplin · Michael Schmid · Anton Hartmann

Received: 26 March 2014 / Revised: 24 June 2014 / Accepted: 24 July 2014  
© Springer-Verlag Berlin Heidelberg 2014

**Abstract** In this interdisciplinary approach, the dynamics of production and degradation of the quorum sensing signal 3-oxo-decanoylhomoserine lactone were studied for continuous cultures of *Pseudomonas putida* IsoF. The signal concentrations were quantified over time by use of monoclonal

antibodies and ELISA. The results were verified by use of ultra-high-performance liquid chromatography. By use of a mathematical model we derived quantitative values for non-induced and induced signal production rate per cell. It is worthy of note that we found rather constant values for different rates of dilution in the chemostat, and the values seemed close to those reported for batch cultures. Thus, the quorum-sensing system in *P. putida* IsoF is remarkably stable under different environmental conditions. In all chemostat experiments, the signal concentration decreased strongly after a peak, because emerging lactonase activity led to a lower concentration under steady-state conditions. This lactonase activity probably is quorum sensing-regulated. The potential ecological implication of such unique regulation is discussed.

**Electronic supplementary material** The online version of this article (doi:10.1007/s00216-014-8063-6) contains supplementary material, which is available to authorized users.

K. Buddrus-Schiemann · M. Rieger · M. Mühlbauer · M. Rothballer · M. Schmid · A. Hartmann (✉)  
Research Unit Microbe-Plant Interactions, Helmholtz Zentrum München, German Research Centre for Environmental Health (GmbH), Ingolstädter Landstrasse 1, 85764 Neuherberg, Germany  
e-mail: anton.hartmann@helmholtz-muenchen.de

M. V. Barbarossa  
Bolyai Institute, University of Szeged, Aradi vértanúk tere 1,  
6720 Szeged, Hungary

C. Kuttler  
Centre for Mathematical Sciences, Technische Universität München,  
Boltzmannstrasse 3, 85748 Garching, Germany

B. A. Hense  
Institute of Computational Biology, Helmholtz Zentrum München,  
German Research Centre for Environmental Health (GmbH),  
Ingolstädter Landstrasse 1, 85764 Neuherberg, Germany

J. Uhl · J. R. Fonseca · P. Schmitt-Kopplin  
Research Unit Analytical BioGeoChemistry, Helmholtz Zentrum München, German Research Centre for Environmental Health (GmbH), Ingolstädter Landstrasse 1, 85764 Neuherberg, Germany

P. Schmitt-Kopplin  
Analytical Food Chemistry, Technische Universität München,  
Alte Akademie 10, 85354 Freising-Weißenstephan, Germany

**Keywords** *Pseudomonas putida* IsoF · Continuous culture · *N*-acylhomoserine lactones · Mathematical modelling · ELISA · Quorum sensing

## Introduction

For an increasing number of bacterial strains, cell-to-cell communication, called quorum sensing (QS) [1], has been reported to be of fundamental importance in adapting to environmental changes. These bacteria regulate gene expression via small diffusible signal molecules, called autoinducers (AI), which are released into the environment [2, 3]. The concentration of signaling molecules in the cell environment increases when the bacterial population density increases. As soon as a specific cell density threshold has been reached, AI molecules bind to a transcriptional regulator that activates

expression of the AI-biosynthesis gene in an auto-inducing manner, and expression of several QS-dependent target genes. AI regulate a variety of bacterial traits, for example biofilm formation, siderophore production, swarming motility, and production of antibiotics or virulence factors [4–8].

Gram-negative bacteria mainly communicate via *N*-acylhomoserine lactones (AHLs) [3, 9], typically produced by a LuxI-type synthase. AHL molecules bind to cytoplasmic LuxR-type receptors, which control the transcription of target genes. The LuxR-AHL complex usually induces expression of LuxI-type AHL synthases in a positive feedback loop. Bacteria can harbor one or more LuxI/LuxR-type systems and mostly synthesize multiple AHLs.

*Pseudomonas putida* IsoF contains only one known QS system (PpuI/PpuR) that regulates the production of different AHLs, including 3-oxo-dodecanoylhomoserine lactone (3-oxo-C12-AHL) and 3-oxo-decanoylhomoserine lactone (3-oxo-C10-AHL) [10]. This strain is a root colonizing plant growth-promoting model organism which has been isolated from the tomato rhizosphere [11]. In previous work with *P. putida* IsoF, production and degradation of AHLs in batch cultures were studied [12]. Maximum concentrations of all detected AHLs were reached in the early logarithmic growth phase, followed by a rapid degradation of AHLs to homoserines (HSs), indicating the presence of extracellular lactonase activity. No known lactonase genes of *P. putida* IsoF have yet been clearly identified, but its genome contains several candidate genes coding for enzymes with a broad range of substrates, potentially including AHLs [12, 18]. The synthesis of AI-degrading enzymes and the existence of AHL modification and degradation have also been reported for other AHL-producing bacteria [13–16].

The batch culture approach has major disadvantages. Changing environmental conditions (e.g. nutrients, waste products), which are reflected by a shift from exponential growth to the stationary phase, may not adequately represent natural conditions, when permanent exchange with the environment occurs, keeping the conditions more constant. QS systems themselves are known to be affected by environmental conditions, e.g. nutrient starvation [17, 18]. For *Pseudomonas aeruginosa* an effect of nutrient conditions on QS activity has been reported [19]. Use of continuous cultivation approaches, as in chemostats, enables better understanding of the interaction of cellular physiology and stress responses with the QS response and its fine tuning.

Different methods of analysis based on chromatography and spectrometry have been used to identify and quantify AHL molecules and their degradation products [12, 20, 21]. Immunoassays are new, very cost-effective, and rapid means of detection and quantification of AHLs and HSs directly in biological samples [22]. Therefore, several monoclonal

antibodies have been developed [23] for use in enzyme-linked immunosorbent assays (ELISAs) that require small amounts of sample and less sample preparation.

In this study, the dynamics of production and degradation of 3-oxo-C10-AHL, the dominant AHL of *P. putida* IsoF, were investigated over time in continuous growth experiments by use of ELISA, ultra-high-performance liquid chromatography (UHPLC), and mathematical modelling. Controlled continuous cultivation enabled reproducible establishment of defined environmental conditions. For quantitative description of the QS system we used mathematical modelling based on ordinary (ODE) and delay differential equations (DDEs). Similar mathematical models have been introduced for batch culture experiments [12, 24].

The main objectives of this study were to analyze whether the QS system of *P. putida* IsoF is quantitatively different from those of other organisms—reflecting possible relevance of environmental factors—and to investigate long-term behavior under conditions not entering the stationary phase.

## Material and methods

### Bacterial strain and medium

*Pseudomonas putida* IsoF [11] was cultivated in ABC minimal medium [25] with sodium citrate ( $10 \text{ mmol L}^{-1}$ ) as carbon source at  $30 \text{ }^{\circ}\text{C}$  with shaking at 200 rpm. The medium was adjusted to pH 6.8 to avoid abiotic degradation of AHLs [26]. The chemicals used were purchased from Sigma–Aldrich (Taufkirchen, Germany). For cultivation of bacterial cell suspensions, an Innova 4200 incubator (New Brunswick Scientific, Edison, NJ, USA) was used.

### Continuous culture conditions

The Biostat Aplus bioreactor system (Sartorius Stedim Biotech, Göttingen, Germany) with a working volume of 2 L was used in this study. All continuous culture (CC) was performed under controlled conditions at  $30 \text{ }^{\circ}\text{C}$ . The pH was maintained at 6.8 and the dissolved oxygen concentration was kept above 50 % air saturation. Three different dilution rates ( $D$ ) of 0.1 (CC1), 0.2 (CC2), and  $0.4 \text{ L h}^{-1}$  (CC3) and a repetition of  $D=0.2$  (rCC2) were used and controlled by medium supply and, simultaneously, medium outflow by use of peristaltic pumps. Before inoculation, the cell density (OD<sub>436 nm</sub>) of an overnight culture was adjusted and the stirred medium was then inoculated 1:1000. Samples were taken directly after inoculation, 6 ( $D 0.1 \text{ L h}^{-1}$ ), 12 ( $D 0.2 \text{ L h}^{-1}$ ), and 16 ( $D 0.4 \text{ L h}^{-1}$ ) hours after inoculation, and then every hour. The three different CCs were run for 39 h ( $D 0.1 \text{ L h}^{-1}$ ), 42 h ( $D 0.2 \text{ L h}^{-1}$ ), and 49 h ( $D 0.4 \text{ L h}^{-1}$ ), respectively.

## Sample preparation

Samples were collected via the outflow by use of an overflow tube connected to a continuously running peristaltic pump. To quantify the cell number of every sample, 10  $\mu\text{L}$  cell suspension was sampled and cells were counted using a microscope (Axioplan; Carl Zeiss, Oberkochen, Germany). Cell number was determined as the mean value from ten randomly chosen counting squares. The cell suspensions were centrifuged at 9,000 rpm and 4  $^{\circ}\text{C}$  for 15 min and the supernatant was filtered through Millipore nitrocellulose filters (0.22  $\mu\text{m}$ , type GSWP), by use of a vacuum pump. The filtered samples were stored at  $-20^{\circ}\text{C}$  until measurement. To control the sterility of the running continuous culture system, 1-mL samples were fixed with paraformaldehyde, fluorescence in situ hybridization was performed as described elsewhere [27], and samples were checked under the microscope.

## ELISA materials and chemicals

Nunc Maxisorp 96-well microtiter plates and lids were purchased from Thermo Fisher Scientific (Schwerte, Germany) and Greiner 96-well U-shape PP low-binding microtiter plates were obtained from Greiner Bio-One (Monroe, LA, USA). Ultra-pure water, which was used for preparation of all buffers and solutions, was obtained from a Milli-Q filter system from Millipore (Eschborn, Germany). Washing of microtiter plates was performed with an automated microtiter plate washer from Bio-Tek Instruments (Bad Friedrichshall, Germany). Absorbance was read by use of a Spectra Max M5<sup>e</sup> multi-detection reader from Molecular Devices (Palo Alto, CA, USA). A Heidolph Instruments Titramax 1000 (Schwabach, Germany) heating–shaking–mixing system was used for incubation or shaking of the microtiter plates.

3,3',5,5'-Tetramethylbenzidine (TMB), dimethyl sulfoxide, 99 % (DMSO), hydrogen peroxide ( $\text{H}_2\text{O}_2$ ) and skimmed milk powder were purchased from Sigma–Aldrich (Steinheim, Germany). Buffer salts and solvents (Tween 20 and sulfuric acid 95–97 %) were purchased from Merck (Darmstadt, Germany). The AHL standard 3-oxo-C10-AHL was obtained from Cayman Chemical (Ann Arbor, MI, USA), dissolved in acetonitrile, and stored at  $-20^{\circ}\text{C}$  to avoid hydrolysis. The HS standard was prepared by stirring an aliquot of the AHL standard with 10 % 1 mol  $\text{L}^{-1}$  NaOH at room temperature (RT) before storing at  $-20^{\circ}\text{C}$  [23]. The rat monoclonal antibody (mAb) HSL1-1A5 with the highest affinity for 3-oxo-C10-AHL was produced in-house (E. Kremmer, Institute of Molecular Immunology, Helmholtz Zentrum München, Neuherberg, Germany), as described elsewhere [23]. As secondary antibody, we used a goat-anti-rat antibody conjugated to horseradish peroxidase (GaR-HRP)

which was obtained from Dianova (Hamburg, Germany). The coating antigen HSL2-BSA-r2 was prepared in-house as reported elsewhere [23].

## Operating procedure for coating antigen ELISA

The operating procedure for coating antigen ELISA was based on previous work [22, 28] and was modified for use in this study. Briefly, high-binding microtiter plates were coated with the AHL coating antigen HSL2-BSA-r2 (0.1  $\mu\text{g mL}^{-1}$ , 100  $\mu\text{L}$  per well) in 50 mmol  $\text{L}^{-1}$  carbonate buffer at 4  $^{\circ}\text{C}$  overnight. The next day, the plates were washed three times with 40 mmol  $\text{L}^{-1}$  phosphate-buffered saline (PBS) containing 0.5 % Tween 20, and free binding places at the surface of the microtiter plate were blocked with skimmed milk powder (1 %, 300  $\mu\text{L}$  per well) in 40 mmol  $\text{L}^{-1}$  PBS for 1 h at RT. During this blocking step, 75  $\mu\text{L}$  per well of each standard solution in ABC minimal medium ( $c(3\text{-oxo-C10-AHL})=0, 1, 10, 50, 100, 500, 1000, 5000, 10000, 50000 \mu\text{g L}^{-1}$  and  $c(3\text{-oxo-C10-HS})=0, 0.01, 0.1, 1, 10, 50, 100, 500, 1000, 10000 \mu\text{g L}^{-1}$ ) and the culture samples in the hydrolyzed (samples treated with 10 % 1 mol  $\text{L}^{-1}$  NaOH for 15 min at RT followed by neutralization with 40  $\mu\text{L}$  1 mol  $\text{L}^{-1}$  HCl and 10  $\mu\text{L}$  ABC medium) and non-hydrolyzed form were preincubated in a low-binding microtiter plate together with the mAb HSL1-1A5 (50 ng  $\text{mL}^{-1}$ , 75  $\mu\text{L}$  per well) in 40 mmol  $\text{L}^{-1}$  PBS. The preincubated mixture of standard or sample and mAb (100  $\mu\text{L}$ ) was then transferred to the blocked and coated plate after washing. This plate was incubated for 1 h at RT, washed, and filled with the secondary Ab GaR-HRP (50 ng  $\text{mL}^{-1}$ , 100  $\mu\text{L}$  per well) in 40 mmol  $\text{L}^{-1}$  PBS containing 0.5 % Tween 20. After subsequent incubation for 1 h at RT and a final washing step, 100  $\mu\text{L}$  per well TMB substrate (200  $\mu\text{L}$  1 %  $\text{H}_2\text{O}_2$ , 800  $\mu\text{L}$  6 mg  $\text{mL}^{-1}$  TMB in DMSO, dissolved in 50 mL 0.1 mol  $\text{L}^{-1}$  sodium acetate buffer, pH 5.5) was added. After 10–20 min, the enzyme reaction was stopped by addition of 50  $\mu\text{L}$  per well 2 mol  $\text{L}^{-1}$  sulfuric acid, and the absorbance at 450 nm (reference 650 nm) was measured with a SpectraMax M5<sup>e</sup> microplate reader (Molecular Devices).

## Calculation of AHL and HS concentrations

Curve fitting of the standard curves was done with SOFTmax Pro 5.2 (Molecular Devices) or SigmaPlot 12.0 (Systat Software, Chicago, IL, USA) by use of a four-variable fitting equation (Eq. 1):

$$y = \frac{A-D}{1 + \left(\frac{x}{C}\right)^B} + D \quad (1)$$

This ELISA was optimized for 3-oxo-C10-AHL as main analyte. Because of the method of production of the mAbs, all obtained mAbs had higher affinity for the HS than for its

corresponding AHL. This cross-reactivity ( $CR$ ) can be calculated by use of Eqs. (2) and (3):

$$CR_{HS} = \frac{IC_{50}(3\text{-oxo-C10-AHL})}{IC_{50}(3\text{-oxo-C10-HS})} \quad (2)$$

$$CR_{AHL} = \frac{IC_{50}(3\text{-oxo-C10-HS})}{IC_{50}(3\text{-oxo-C10-AHL})} \quad (3)$$

The  $CR$ s were calculated for each microtiter plate and used for calculation of AHL and HS concentrations in samples from the same microtiter plate. To calculate AHL and HS concentrations simultaneously, culture samples in the non-hydrolyzed and hydrolyzed forms were referred to standard curves for AHL and HS. Regarding the AHL standard curve, the signal of the non-hydrolyzed sample ( $S(AHL)_{\text{non-hydrolyzed}}$ ), which can be described as AHL-equivalents [22], results from the AHL concentration and the HS concentration multiplied by its  $CR$  (Eq. 4):

$$S(AHL)_{\text{non-hydrolyzed}} = c(AHL) + c(HS) \times CR_{HS} \quad (4)$$

We verified that all AHL molecules were degraded to HS molecules in the hydrolyzed culture samples (data not shown). Therefore, the signal for the hydrolyzed sample ( $S(AHL)_{\text{hydrolyzed}}$ ) results from the sum of AHL and HS concentration multiplied by its  $CR$  (Eq. 5):

$$S(AHL)_{\text{hydrolyzed}} = [c(AHL) + c(HS)] \times CR_{HS} \quad (5)$$

Regarding the HS standard curve, the signal of the non-hydrolyzed sample ( $S(HS)_{\text{non-hydrolyzed}}$ ) results from the AHL concentration multiplied by its  $CR_{AHL}$  and the HS concentration (Eq. 6):

$$S(HS)_{\text{non-hydrolyzed}} = c(HS) + c(AHL) \times CR_{AHL} \quad (6)$$

The signal for the hydrolyzed sample ( $S(HS)_{\text{hydrolyzed}}$ ) results from the sum of the AHL and HS concentrations (Eq. 7):

$$S(HS)_{\text{hydrolyzed}} = c(AHL) + c(HS) \quad (7)$$

With these formulas, we calculated the AHL and HS concentrations by use of Eqs. (8) and (9):

$$c(AHL) = \frac{S(AHL)_{\text{hydrolyzed}} - S(AHL)_{\text{non-hydrolyzed}}}{CR_{HS} - 1} \quad (8)$$

$$c(HS) = S(HS)_{\text{non-hydrolyzed}} - c(AHL) \times CR_{AHL} \quad (9)$$

#### Quantitative analyses of AHL by UHPLC-MS

Sample pre-treatment before chemical analysis is usually required to isolate AHLs from cell culture samples. Therefore,

solid-phase extraction (SPE) was performed using hybrid magnetic microparticles (HMP) [29, 30]. Magnetic iron oxide nanospheres were produced on the surface of an adsorbent material by solvothermal reduction of iron(III) [31]. In a glass vial, 0.270 g  $FeCl_3$  (Santa Cruz Biotechnology, Heidelberg, Germany) and 0.700 g sodium acetate (Merck, Darmstadt, Germany) were dissolved in 8 mL ethylene glycol (Serva Electrophoresis, Heidelberg, Germany) in an ultrasonic bath for 5 min. Microparticles of the copolymer Oasis HLB (hydrophilic-lipophilic-balanced reversed-phase sorbent; Waters, Milford, MA, USA; 100 mg) were then added and the solution was stirred until it became homogenous. To produce hybrid magnetic particles, the vial was sealed in a Teflon-lined stainless-steel digestion vessel (Parr Instrument, Frankfurt, Germany) and maintained in an oven for 12 h at 200 °C. Finally, the synthesized HMP were separated from the reaction solvent by use of an external magnet then washed with purified water ( $5 \times 5$  mL) then methanol ( $5 \times 5$  mL). HMP were then dried at 60 °C. The production process was repeated to generate enough HMP to perform the experiment. Also, HMP from different batches were mixed and homogenized before application.

In a test tube, 25 mg HMP was first weighed then conditioned with 1 mL methanol and 1 mL purified water. AHL extraction was performed by adding 2.5 mL cell culture supernatant to the tube, incubating it at room temperature for 20 min, for interaction, stirring occasionally to ensure good mixing. HMP were then captured at the edge of the tube by use of an external magnet, so supernatant was easily discarded. HMP were then washed with 2 mL purified water, followed by elution of the AHLs with 2 mL 3-propanol-hexane (75:25 %v/v) [21]. Eluates were dried in a centrifugal vacuum concentrator (Savant SPD121P SpeedVac Concentrator; Thermo Fisher Scientific, Langenselbold, Germany) and re-dissolved in 250  $\mu$ L acetonitrile-water (10:90 %v/v).

To construct a calibration curve, standard solutions of 3-oxo-C10-AHL (University of Nottingham, Nottingham, UK) in the concentration range 0.01–0.50 mg L<sup>-1</sup> were freshly prepared in ABC minimal medium before chemical analysis. Thus, AHL extraction using HMP was performed by following the same procedure as used for cell culture samples.

Quantitative measurements were performed by use of an Acquity UPLC System (Waters Corporation, Milford, MA, USA) coupled to a quadrupole time-of-flight mass spectrometer equipped with an Apollo II electrospray ionization source (ESI-qTOF MS; maXis; Bruker Daltonik, Bremen, Germany). Chromatographic separation was achieved on a 1.0 mm  $\times$  150 mm Acquity BEH C18 column packed with a 1.7  $\mu$ m particles (Waters Corporation, Milford, MA, USA). The sample manager temperature was set to 10 °C and 5  $\mu$ L sample was injected through a partial loop. The mobile phase was a gradient prepared from water containing 10 % acetonitrile and 0.1 % formic acid (component A) and 100 % acetonitrile

(component B). Linear gradient elution was applied from 0 % to 90 % B in 5 min; the flow rate was 0.100 mL min<sup>-1</sup>. Mass spectra were acquired in positive ionization mode within the mass range 50–1000 *m/z*. All samples were measured as duplicate. Chromatograms and mass spectra acquired from UHPLC-ESI-qTOF MS measurements were processed with Data Analysis 3.4 software (Bruker Daltonik, Bremen, Germany).

### Mathematical modelling

The mathematical modelling approach used in this study was based on delay differential equations (DDEs), which enable past states to be included in the dynamics of the system. We used variables for the substrate concentration (*S*), bacterial cell density (*N*), AHL concentration (*A*), the AHL-degrading lactonase concentration (*L*), and intracellular PpuR-AHL complex concentration (*C*). Their dynamics were described by differential equations. A schematic diagram of the QS regulation system in the cytoplasm is given in Fig. 1b. Figure 1a shows the dynamics during continuous culture with medium inflow, and outflow of substrate, cells, and other molecules.

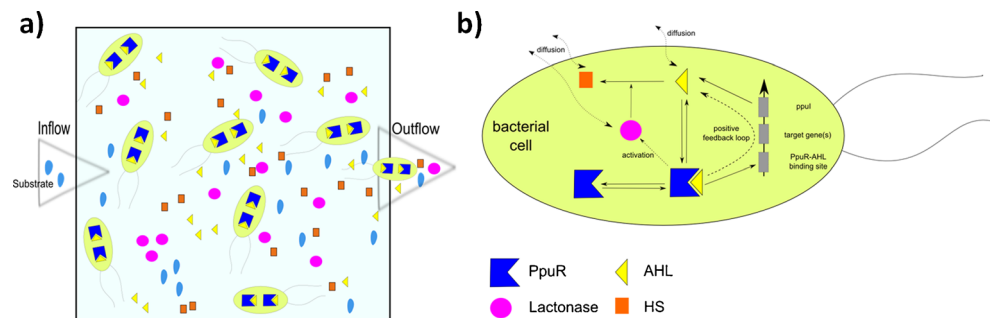
In the following text, we briefly introduce the mathematical model (Eqs. 10–14). More details can be found in the [Electronic Supplementary Material \(ESM\)](#).

$$S'(t) = \underbrace{DS_0}_{\text{inflow}} - \underbrace{\gamma_S N(t) \frac{S(t)^{n_s}}{K_m^{n_s} + S(t)^{n_s}}}_{\text{substrate consumption}} - \underbrace{DS(t)}_{\text{outflow}} \quad (10)$$

$$N'(t) = \underbrace{aN(t) \frac{S(t)^{n_s}}{K_m^{n_s} + S(t)^{n_s}}}_{\text{nutrient-regulated cell division}} - \underbrace{DN(t)}_{\text{outflow}} \quad (11)$$

$$A'(t) = \underbrace{\left( \alpha_A + \beta_A \frac{C(t)^{n_1}}{C_1^{n_1} + C(t)^{n_1}} \right) N(t)}_{\text{AHL production}} - \underbrace{\gamma_A A(t)}_{\text{abiotic decay}} - \underbrace{\alpha_C (R_{\text{const}} - C(t)) A(t)}_{\text{complex formation}} + \underbrace{\gamma_3 C(t)}_{\text{complex decomposition}} - \underbrace{DA(t)}_{\text{washout}} - \underbrace{K_E A(t) L(t)}_{\text{lactonase-regulated degradation}} \quad (12)$$

**Fig. 1** Schematic representation of the quorum sensing regulation system for a single bacterial cell (b) and the conditions in the continuous culture vessel (a) as basis for the mathematical model



$$C'(t) = \underbrace{\alpha_C (R_{\text{const}} - C(t)) A(t)}_{\text{complex formation}} - \underbrace{\gamma_3 C(t)}_{\text{complex decomposition}} \quad (13)$$

$$L'(t) = \underbrace{\alpha_L \frac{C(t-\tau)^{n_2}}{C_2^{n_2} + C(t-\tau)^{n_2}} N(t)}_{\text{lactonase production}} - \underbrace{\gamma_L L(t)}_{\text{abiotic decay}} - \underbrace{DL(t)}_{\text{washout}} \quad (14)$$

Nutrient consumption and cell growth were described by the standard approach for a continuous culture [32]. Similar to Fekete et al. [12], we included a positive feedback loop for AHL regulation. Similarly, lactonase activity was regulated by the PpuR-AHL complex with a specific time delay [24]. In contrast with the modelling approach of Fekete et al. [12], we considered also a time-dependent variable for the PpuR-AHL complex to obtain a more refined model.

Fitting was mainly performed by use of “fminsearch” in the software MATLAB (MathWorks, Ismaning, Germany), a method based on the simplex search algorithm. The model variables are listed in Table 1.

### Results and discussion

#### Quantitative analysis of AHL molecules in continuous cultures

In contrast with routinely used batch cultures, which have shifting conditions among lag phase, logarithmic phase, and stationary phase, continuous culture experiments enable reproducible establishment of steady state growing conditions with different concentrations of substrates and different cell densities at different supplied dilution rates and/or growth rates. We were able to investigate the production and degradation of AHL by *P. putida* IsoF grown in continuous cultures with three different dilution rates of 0.1, 0.2, and 0.4 L h<sup>-1</sup>.

For quantification of 3-oxo-C10-AHL by ELISA, each standard or sample was measured in triplicate, which enables simultaneous quantification of AHL and HS concentrations in six samples on one microtiter plate. For this study, four continuous cultures with up to 30 samples were examined by ELISA, resulting in a set of 24 standard curves for AHL and

**Table 1** Variables used in the model equations

Symbol	Description
$N(t)$	Cell density at time $t$ (cells $L^{-1}$ )
$S(t)$	Substrate concentration at time $t$ (U)
$A(t)$	AHL concentration in medium at time $t$ (mol $L^{-1}$ )
$C(t)$	PpuR-AHL concentration in one cell at time $t$ (mol $L^{-1}$ )
$L(t)$	Lactonase concentration in medium at time $t$ (mol $L^{-1}$ )
$\tau$	Delay in lactonase activation (h)
$D$	Chemostat inflow/outflow rate ( $h^{-1}$ )
$a$	Cell division rate ( $h^{-1}$ )
$\gamma_S$	Nutrient consumption rate (U L per cell $h^{-1}$ )
$K_m$	Substrate conc. at which half max. consumption rate is reached (U)
$n_s$	Nonlinearity in substrate consumption process (dimensionless)
$\alpha_A$	Basic AHL production rate (mol per cell $L^{-1}$ )
$\beta_A$	PpuR-AHL regulated AHL production rate (mol per cell $L^{-1}$ )
$n_1$	Polymerization degree for PpuR-AHL (in AHL production process) (dimensionless)
$C_1$	Threshold value for PpuR-AHL concentration (in AHL production process) (mol $L^{-1}$ )
$\gamma_A$	AHL degradation rate ( $h^{-1}$ )
$\alpha_c$	Binding rate for PpuR-AHL (L mol $^{-1}$ $h^{-1}$ )
$\gamma_3$	PpuR-AHL degradation rate (backwards reaction) ( $h^{-1}$ )
$R_{const}$	Total PpuR concentration in the cells (mol $L^{-1}$ )
$K_E$	AHL degradation rate (lactonase-regulated) (L mol $^{-1}$ $h^{-1}$ )
$\alpha_L$	Lactonase activation/production rate (mol per cell $h^{-1}$ )
$\gamma_L$	Lactonase degradation rate ( $h^{-1}$ )
$C_2$	Threshold value for PpuR-AHL concentration (in lactonase activation) (mol $L^{-1}$ )
$n_2$	Polymerization degree for PpuR-AHL (in lactonase activation process) (dimensionless)

HS. Representative examples of typical AHL and HS standard curves are shown in Fig. 2. As working range (WR) of the ELISAs, 85 % to 15 % of the maximum signal was taken [33]. With this definition the mean WR of the ELISA, in ABC medium, was determined to be  $187 \pm 75$  to  $1806 \pm 487$   $\mu g L^{-1}$  for 3-oxo-C10-AHL and  $13 \pm 7$  to  $278 \pm 166$   $\mu g L^{-1}$  for 3-oxo-C10-HS.

3-oxo-C10-AHL concentrations were also determined by UHPLC–MS, with monitoring of the ion  $m/z$  270.1707  $[M+H]^+$  with high accuracy and use of the extracted ion chromatogram (EIC) to calculate the peak area. The peak retention time was 3.9 min and the calibration curve showed linearity was good within the concentration range 0.01–0.5  $mg L^{-1}$ , with a coefficient of determination of 0.9918. In Fig. 3a calculated concentrations are plotted against sampling time for one continuous culture. The results confirmed the ELISA measurements for AHL concentration.

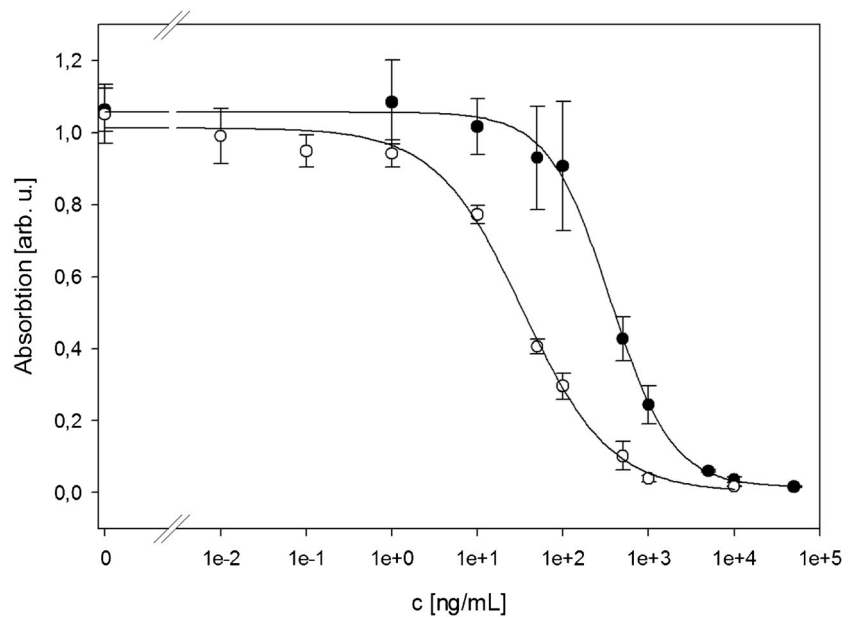
Cell density and 3-oxo-C10-AHL concentration had qualitatively similar dynamics for dilution rates of 0.2, 0.1, and

0.4  $L h^{-1}$  (Fig. 3a–c). Sigmoid growth of the bacteria population was observed after inoculation. Similarly, the 3-oxo-C10-AHL concentration increased after a delay (note that in some experiments a non-zero concentration of 3-oxo-C10-AHL was obtained at  $t=0$ , probably because of the induced state in the stock culture). Interestingly, at approximately the time when cell density approaches equilibrium, the 3-oxo-C10-AHL concentrations in all experiments declined sharply and seemed to approach a low equilibrium level.

In a next step, results were estimated by fitting the mathematical model to the experimental data (Table 2). First, the model was fitted to the data of experiment CC2 (Fig. 3a). The values obtained were used to check their predictive value for CC1 and CC3, which fitted quite well (Fig. 3b, c). Minor adaptations for a few values only, especially some initial values, increased the quality of the fit. Although the measured data vary (probably mainly because of noise), the resulting model were a good match with the general data trends. Hence, except for the starting values at  $t=0$ , most values can be chosen identically, i.e., irrespective of the chosen dilution rates (this also applied for the repetition experiment of  $D=0.2 L h^{-1}$  (rCC2; ESM Fig. S2). QS results (basic and induced AHL production rate and AHL induction threshold concentration) identical with those used here have been reported for experiments on *P. putida* IsoF under batch culture conditions [12]. The results are, furthermore, consistent with microfluidic experiments with attached microcolonies (although evidence in these experiments was more indirect) [34]. There are also no clear indications of shifts of other values related to QS as a function of dilution rate. A possible exception may be the total cellular PpuR concentration  $R_{const}$ , which has a tendency to increase with increasing dilution rate. Thus, at least for the range of conditions investigated, the induction behavior of *P. putida* IsoF is surprisingly stable.

Nutrient depletion is greater in experiments with lower dilution rates. The model indicates substrate concentration at equilibrium of approximately 6 % of the inflow concentration for  $D=0.1 L h^{-1}$  compared with 26 % for  $D=0.4 L h^{-1}$ . It remains unclear whether the different total PpuR concentrations may be connected with this. Regulation of the AHL receptor in response to environmental stress has been reported for other species. For *V. fischeri*, stress upregulates the concentration of the AHL receptor LuxR [35]. *Pseudomonas aeruginosa* responds to phosphor starvation by upregulating production of RhIR [19]. Compared with *V. fischeri* and *P. aeruginosa*, our chemostat experiments are indicative of an inverse correlation between starvation stress and AHL receptor concentration for *P. putida* (lower nutrient stress is connected with higher PpuR concentration). For *V. fischeri*, the relationship between QS system and stress was reported depend on the degree of starvation, i.e. at intermediary nutrient stress levels QS activity increases whereas at very severe starvation QS activity is downregulated [36].

**Fig. 2** Representative examples of ELISA standard curves for 3-oxo-C10-AHL (open circles) and 3-oxo-C10-HS (filled circles)



To explain the sharp decline of AHL concentration after the peak, even an abrupt and complete stop of AHL production in the model was insufficient (not shown)—increased degradation was needed. The AHL concentrations indicate the activity of a lactonase. Fekete et al. [12] reported that induction of lactonase activity was not connected with entering the stationary state, but occurred during the logarithmic growth phase. Our chemostat studies confirmed this finding. The degradation of AHL by a lactonase revealed no clear tendency to shift in correlation with different dilution rates. Thus, at least for our range of environmental conditions, neither environmental conditions, for example nutrient depletion, nor growth rates (which vary in equilibrium between approx.  $0.05$  and  $0.2 \text{ h}^{-1}$ , according to the given dilution rates) seem to be the dominating factors inducing lactonase expression. We conclude that, in accordance with batch culture results, lactonase production under chemostat conditions is probably controlled by QS.

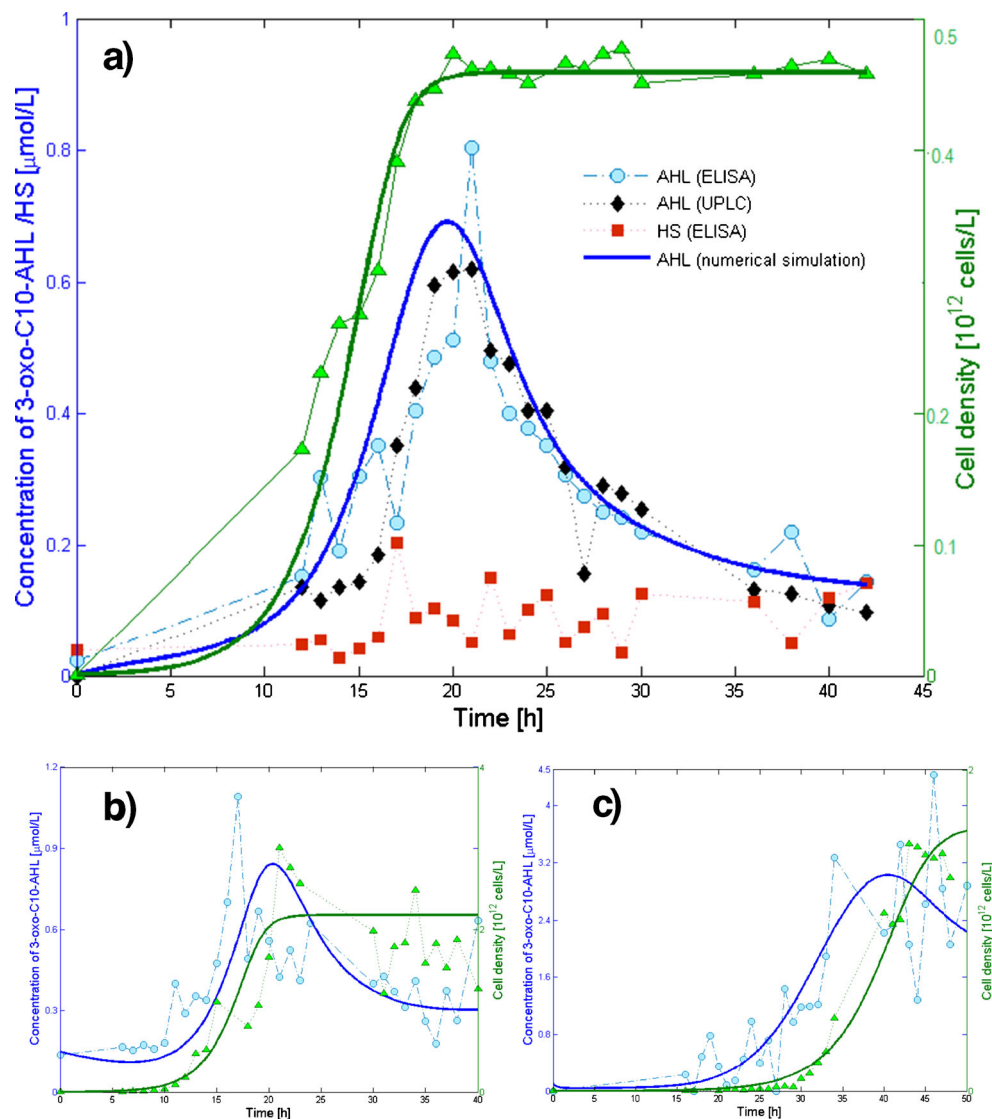
The genes coding for this lactonase remain to be identified. In their study, Fekete et al. [12] suggested some candidate genes coding for enzymes with more promiscuous substrate specificity which, with other substrates, also cleave different types of AHL molecule (metallo- $\beta$ -lactamase, phosphodiesterase, gluconolactonase and phosphogluconolactonase). As far as we are aware, no such lactonase activity has yet been demonstrated for *P. aeruginosa* PAO1, although the presence of several acylase genes has been reported [15]. However, some of these acylases, which degrade AHLs not by cleaving the lactone ring but the acyl side chain, only had a slight modulatory effect on AHL concentration compared with wild-type to *P. aeruginosa* acylase negative mutants and seem to be restricted to long-chain AHL only [15]. On the transcriptional level, except for RsaL no other negative regulators have yet been found in the genomes of *P. putida* strains. Moreover,

unlike *P. aeruginosa* RsaL activity, for *P. putida* WCS 358 an additional molecule repressing *ppuI* transcription has been postulated, which might link this mechanism to other environmental or physiological conditions in the cell [37]. Homologues with other transcriptional regulators, for example the recently reported QteE and QscR [38], could not be found in any of the available genomes of *P. putida* strains (data not shown). Therefore the QS control via lactonase activity on a posttranscriptional level can be regarded as important for *P. putida* IsoF because it is lacking the tight transcriptional regulation of QS found for *P. aeruginosa* [38].

Our fitted model curves seem to indicate that the system approaches an equilibrium, in which both induced AHL production and lactonase production co-exist. However, from the perspective of cost-efficiency and ecological purpose this is difficult to explain. One alternative could be a changed rate of AHL production after onset of the lactonase effect. We approached this question in a simplified model, containing no positive feedback of AHL induction (i.e.,  $\beta A = 0$ ), and no lactonase. This approach revealed for all dilutions a similar “equilibrium net production rate” of approximately  $3 \times 10^{-20} \text{ mol per cell h}^{-1}$ . Thus, although the 3-oxo-C10-AHL concentration remained above the threshold concentration for QS induction in all experiments, the net rate of production not only falls below the induced production ( $\alpha A + \beta A$ ), but even below the basic production  $\alpha A$  by approximately one order of magnitude.

These AI dynamics observed for *P. putida* IsoF clearly contradict the usual assumption of induced AHL production as long as the population density exceeds a specific threshold and does not enter the stationary phase in a batch culture. Of course, the proposed down-regulation would most likely require a modulatory mechanism on the transcriptional level,

**Fig. 3** Experimental data and numerical simulations (continuous curves) for continuous culture with dilution rates of (a)  $0.2 \text{ L h}^{-1}$  (CC2), (b)  $0.1 \text{ L h}^{-1}$  (CC1), and (c)  $0.4 \text{ L h}^{-1}$  (CC3). Bacterial cell density (triangles), ELISA-based (circles) and UHPLC-based (diamonds, only for CC2) 3-oxo-C10-AHL concentrations and ELISA-based 3-oxo-C10-HS concentrations (squares, only for CC2) in *Pseudomonas putida* IsoF culture supernatant. Standard deviations of measured data are excluded from the figures for reasons of clarity, but were  $<20\%$ . The values used for this numerical simulation are given in Table 2



quite similar to the environment-dependent activity postulated for RsaL for *P. putida* WCS 358. To address this question transcriptional analysis under different environmental conditions would be necessary.

Alternatively, the QS system could work in an oscillating manner, e.g. to enable a kind of periodical reset. Because of the low rate of abiotic degradation of AHLs at pH around and below 7.0 [26], the cells are exposed to AHL concentrations which reflect not only the actual cell density but also that in the past. This may not be desirable for actual decisions. Periodic degradation would diminish the impact of the past in a reset button-like way. The regulation system of *P. putida* IsoF consists of positive feedback (AHL promoted AHL synthesis) coupled with negative feedback (via lactonase). Depending on the conditions, such a system can, indeed, oscillate with a period longer than the duration of our experiment [39]. Note that this hypothesis does not require altered values of  $\alpha_A$  and

$\beta_A$ , because the decline of AHL concentration could be because of changing lactonase only.

Finally, a change of conditions (e.g. cell density) rather than the actual state is often of relevance for signal-receiver systems. QS systems which use waste products of central metabolic pathways (e.g. AI-2), intrinsically take this into account, because the rate of growth is usually coupled to metabolic activity. It is generally agreed that AHLs and their precursors are not metabolic waste products. Nevertheless, although the potential mechanism behind such a strategy is not clear for AHL, a low net rate of production under approximately constant cell density conditions fits this idea.

To summarize, the chemostat experiment significantly widened our perception of the functionality of the QS system of *P. putida* IsoF, although many of the results are difficult to interpret ecologically on the basis of current knowledge. Additional experiments, e.g. with longer observation times

**Table 2** Model values for CC1, CC2, rCC2, and CC3

Symbol	Value (CC1)	Value (CC2)	Value (rCC2)	Value (CC3)
$S(0)$ (U)	1	1	1	1
$N(0)$ (cells L <sup>-1</sup> )	$1.5 \times 10^9$	$8.4 \times 10^8$	$8 \times 10^8$	$1.8 \times 10^8$
$A(0)$ (mol L <sup>-1</sup> )	$1.5 \times 10^{-7}$	$2.5 \times 10^{-9}$	$5 \times 10^{-8}$	$1 \times 10^{-8}$
$C(0)$ (mol L <sup>-1</sup> )	$4.9 \times 10^{-8}$	$7.6 \times 10^{-8}$	$6.5 \times 10^{-8}$	$8.2 \times 10^{-8}$
$L(0)$ (mol L <sup>-1</sup> )	$2 \times 10^{-15}$	$5 \times 10^{-15}$	$5 \times 10^{-15}$	$5 \times 10^{-15}$
$\tau$ (h)	2	2	2	2
D (h <sup>-1</sup> )	0.05	0.1	0.1	0.2
a (h <sup>-1</sup> )	0.60	0.66	0.66	0.56
$\gamma_S$ (U L per cell h <sup>-1</sup> )	$2.6 \times 10^{-13}$	$1.3 \times 10^{-12}$	$2.5 \times 10^{-13}$	$2.5 \times 10^{-13}$
$K_m(U)$	0.38	0.38	0.42	0.41
$n_s$ (dimensionless)	1.3	1.3	1.2	1.3
$\alpha_A$ (mol per cell L <sup>-1</sup> )	$2.3 \times 10^{-19}$	$2.3 \times 10^{-19}$	$2.3 \times 10^{-19}$	$2.3 \times 10^{-19}$
$\beta_A$ (mol per cell L <sup>-1</sup> )	$2.3 \times 10^{-18}$	$2.3 \times 10^{-18}$	$2.3 \times 10^{-18}$	$2.3 \times 10^{-18}$
$n_1$ (dimensionless)	2.3	2.3	2.3	2.3
$C_1$ (mol L <sup>-1</sup> )	$70 \times 10^{-9}$	$70 \times 10^{-9}$	$70 \times 10^{-9}$	$70 \times 10^{-9}$
$\gamma_A$ (h <sup>-1</sup> )	0.05	0.05	0.05	0.05
$\alpha_c$ (L mol <sup>-1</sup> h <sup>-1</sup> )	$3 \times 10^4$	$4 \times 10^4$	$4 \times 10^4$	$4 \times 10^4$
$\gamma_\beta$ (h <sup>-1</sup> )	0.080	0.080	0.080	0.080
$R_{const}$ (mol L <sup>-1</sup> )	$8.5 \times 10^{-8}$	$5 \times 10^{-7}$	$5 \times 10^{-7}$	$4 \times 10^{-5}$
$K_E$ (L mol h <sup>-1</sup> )	$2.5 \times 10^{-4}$	$1.5 \times 10^{-4}$	$1.5 \times 10^{-4}$	$2.5 \times 10^{-4}$
$\alpha_L$ (mol per cell h <sup>-1</sup> )	$1.1 \times 10^{-8}$	$1.1 \times 10^{-8}$	$1.1 \times 10^{-8}$	$1.1 \times 10^{-8}$
$\gamma_L$ (h <sup>-1</sup> )	0.005	0.005	0.005	0.005
$C_2$ (mol h <sup>-1</sup> )	$70 \times 10^{-9}$	$70 \times 10^{-9}$	$70 \times 10^{-9}$	$70 \times 10^{-9}$
$n_2$ (dimensionless)	2.5	2.5	2.5	2.5

or different conditions must be conducted. For an increasing number of species with QS systems, the presence of genes coding for enzymes potentially degrading their own AI are known [13–16]. The dynamics of the interplay between QS and these enzymes under different conditions, and thus their ecological purpose, remain obscure. Degradation of butanoylhomoserine lactone (C4-AHL) by *P. aeruginosa* and of 3-oxo-octanoylhomoserine lactone by *Agrobacterium tumefaciens* have been reported to occur during the transition to the stationary phase or in the stationary phase [40–42], but without any indication of AI control of the degrading enzymes. Unfortunately, changing environmental conditions during batch culture experiments impede unambiguous understanding of the mechanisms controlling the enzymes in these studies. Their ecological purpose is usually assumed to be connected with cooperative activity in the stationary phase. However, our chemostat experiment clearly indicates that *P. putida* IsoF AHL is degraded as the cells continue to grow. Although environmental factors, for example nutrients, are known to control expression of genes involved in AI release and of AI receptors, their involvement in the control of degrading enzymes remains unclear. The corresponding results for AI-regulated lactonase for *P. putida* IsoF in batch and chemostat experiments indicate at least some robustness

of lactonase induction under different environmental conditions [12].

Because of a lack of experimental results, the situation is even less clear under biofilm conditions. For *P. aeruginosa*, at least, the quorum sensing activity initially induced decreases with further growth of biofilms, although the number of cells increases [43]. The extent to which AI-degrading enzymes contribute to this counterintuitive result remains unknown.

Furthermore, the relevance of heterogeneity to QS, i.e., with regard to the development of subpopulations among isogenic populations, is increasingly recognized [44]. However, the dynamics of development of heterogeneity among growing populations is poorly understood. For example, we do not know whether AHL-producing and degrading cells belong to the same (sub)population.

**Acknowledgments** We enormously appreciated the great dedication to immunochemical analysis of AHL compounds of Dr Petra Krämer, who died unexpectedly in the early phase of these experiments. Furthermore we want to thank Dr Elisabeth Kremmer, Institute of Molecular Immunology, Helmholtz Zentrum München, for providing the monoclonal antibodies. Maria Vittoria Barbarossa was supported by ERC starting grant no. 259559.

## References

- Fuqua WC, Winans SC, Greenberg EP (1994) Quorum sensing in bacteria: the LuxR-LuxI family of cell density-responsive transcriptional regulators. *J Bacteriol* 176(2):269–275
- Hartmann A, Schikora A (2012) Quorum sensing of bacteria and trans-kingdom interactions of N-acyl homoserine lactones with eukaryotes. *J Chem Ecol* 38(6):704–713. doi:10.1007/s10886-012-0141-7
- Williams P, Winzer K, Chan WC, Cámara M (2007) Look who's talking: communication and quorum sensing in the bacterial world. *Phil Trans R Soc B Biol Sci* 362(1483):1119–1134. doi:10.1098/rstb.2007.2039
- Huber B, Riedel K, Hentzer M, Heydorn A, Gotschlich A, Givskov M, Molin S, Eberl L (2001) The cep quorum-sensing system of *Burkholderia cepacia* H111 controls biofilm formation and swarming motility. *Microbiology* 147(Pt 9):2517–2528
- Koiv V, Mae A (2001) Quorum sensing controls the synthesis of virulence factors by modulating *rsmA* gene expression in *Erwinia carotovora* subsp. *carotovora*. *Mol Gen Genomics* 265(2):287–292. doi:10.1007/s004380000413
- Shih P-C, Huang C-T (2002) Effects of quorum-sensing deficiency on *Pseudomonas aeruginosa* biofilm formation and antibiotic resistance. *J Antimicrob Chemother* 49(2):309–314. doi:10.1093/jac/49.2.309
- Yazgan A, Özcengiz G, Marahiel MA (2001) Tn10 insertional mutations of *Bacillus subtilis* that block the biosynthesis of bacilysin. *Biochim Biophys (BBA) Gene Struct Expr* 1518(1–2):87–94. doi:10.1016/S0167-4781(01)00182-8
- Sokol PA, Malott RJ, Riedel K, Eberl L (2007) Communication systems in the genus *Burkholderia*: global regulators and targets for novel antipathogenic drugs. *Future Microbiol* 2(5):555–563. doi:10.2217/17460913.2.5.555
- Cooley M, Chhabra SR, Williams P (2008) N-acylhomoserine lactone-mediated quorum sensing: a twist in the tail and a blow for host immunity. *Chem Biol* 15(11):1141–1147. doi:10.1016/j.chembiol.2008.10.010
- Steidle A, Allesen-Holm M, Riedel K, Berg G, Givskov M, Molin S, Eberl L (2002) Identification and characterization of an N-acylhomoserine lactone-dependent quorum-sensing system in *Pseudomonas putida* strain IsoF. *Appl Environ Microbiol* 68(12):6371–6382. doi:10.1128/aem.68.12.6371-6382.2002
- Steidle A, Sigl K, Schuegger R, Ihring A, Schmid M, Gantner S, Stoffels M, Riedel K, Givskov M, Hartmann A, Langebartels C, Eberl L (2001) Visualization of N-acylhomoserine lactone-mediated cell-cell communication between bacteria colonizing the tomato rhizosphere. *Appl Environ Microbiol* 67(12):5761–5770
- Fekete A, Kuttler C, Rothballer M, Hense BA, Fischer D, Buddrus-Schiemann K, Lucio M, Müller J, Schmitt-Kopplin P, Hartmann A (2010) Dynamic regulation of N-acyl-homoserine lactone production and degradation in *Pseudomonas putida* IsoF. *FEMS Microbiol Ecol* 72(1):22–34. doi:10.1111/j.1574-6941.2009.00828.x
- Krysciak D, Schmeisser C, Preuß S, Riethausen J, Quitschau M, Grond S, Streit WR (2011) Involvement of multiple loci in quorum quenching of Autoinducer I molecules in the nitrogen-fixing symbiont *Rhizobium (Sinorhizobium)* sp. strain NGR234. *Appl Environ Microbiol* 77(15):5089–5099. doi:10.1128/aem.00112-11
- Uroz S, Oger PM, Chapelle E, Adeline M-T, Faure D, Dessaux Y (2008) A *Rhodococcus qsdA*-encoded enzyme defines a novel class of large-spectrum quorum-quenching lactonases. *Appl Environ Microbiol* 74(5):1357–1366. doi:10.1128/aem.02014-07
- Wahjudi M, Papaioannou E, Hendrawati O, van Assen AHG, van Merkerk R, Cool RH, Poelarends GJ, Quax WJ (2011) PA0305 of *Pseudomonas aeruginosa* is a quorum quenching acylhomoserine lactone acylase belonging to the Ntn hydrolase superfamily. *Microbiology* 157(7):2042–2055. doi:10.1099/mic.0.043935-0
- Yates EA, Philipp B, Buckley C, Atkinson S, Chhabra SR, Sockett RE, Goldner M, Dessaux Y, Cámara M, Smith H, Williams P (2002) N-acylhomoserine lactones undergo lactonolysis in a pH-, temperature-, and acyl chain length-dependent manner during growth of *Yersinia pseudotuberculosis* and *Pseudomonas aeruginosa*. *Infect Immun* 70(10):5635–5646. doi:10.1128/iai.70.10.5635-5646.2002
- Dunlap PV (1999) Quorum regulation of luminescence in *Vibrio fischeri*. *J Mol Microbiol Biotechnol* 1(1):5–12
- De Lay N, Gottesman S (2009) The Crp-activated small noncoding regulatory RNA CyaR (RyeE) links nutritional status to group behavior. *J Bacteriol* 191(2):461–476. doi:10.1128/jb.01157-08
- Mellbye B, Schuster M (2014) Physiological framework for the regulation of quorum sensing-dependent public goods in *pseudomonas aeruginosa*. *J Bacteriol* 196(6):1155–1164
- Fekete A, Frommberger M, Rothballer M, Li X, Englmann M, Fekete J, Hartmann A, Eberl L, Schmitt-Kopplin P (2007) Identification of bacterial N-acylhomoserine lactones (AHLs) with a combination of ultra-performance liquid chromatography (UPLC), ultra-high-resolution mass spectrometry, and in-situ biosensors. *Anal Bioanal Chem* 387(2):455–467. doi:10.1007/s00216-006-0970-8
- Li X, Fekete A, Englmann M, Götz C, Rothballer M, Frommberger M, Buddrus K, Fekete J, Cai C, Schröder P, Hartmann A, Chen G, Schmitt-Kopplin P (2006) Development and application of a method for the analysis of N-acylhomoserine lactones by solid-phase extraction and ultra high pressure liquid chromatography. *J Chromatogr A* 1134(1–2):186–193. doi:10.1016/j.chroma.2006.09.047
- Chen X, Buddrus-Schiemann K, Rothballer M, Krämer P, Hartmann A (2010) Detection of quorum sensing molecules in *Burkholderia cepacia* culture supernatants with enzyme-linked immunosorbent assays. *Anal Bioanal Chem* 398(6):2669–2676. doi:10.1007/s00216-010-4045-5
- Chen X, Kremmer E, Gouzy M-F, Clausen E, Starke M, Wöllner K, Pfister G, Hartmann A, Krämer P (2010) Development and characterization of rat monoclonal antibodies for N-acylated homoserine lactones. *Anal Bioanal Chem* 398(6):2655–2667. doi:10.1007/s00216-010-4017-9
- Barbarossa MV, Kuttler C, Fekete A, Rothballer M (2010) A delay model for quorum sensing of *Pseudomonas putida*. *Biosystems* 102(2–3):148–156
- Clark DJ, Maaløe O (1967) DNA replication and the division cycle in *Escherichia coli*. *J Mol Biol* 23:99–112
- Englmann M, Fekete A, Kuttler C, Frommberger M, Li X, Gebefügi I, Fekete J, Schmitt-Kopplin P (2007) The hydrolysis of unsubstituted N-acylhomoserine lactones to their homoserine metabolites: analytical approaches using ultra performance liquid chromatography. *J Chromatogr A* 1160(1–2):184–193
- Buddrus-Schiemann K, Schmid M, Schreiner K, Welzl G, Hartmann A (2010) Root colonization by *Pseudomonas* sp. DSMZ 13134 and impact on the indigenous rhizosphere bacterial community of barley. *Microb Ecol* 60(2):381–393
- Wöllner K, Chen X, Kremmer E, Krämer PM (2010) Comparative surface plasmon resonance and enzyme-linked immunosorbent assay characterisation of a monoclonal antibody with N-acyl homoserine lactones. *Anal Chim Acta* 683(1):113–118
- Sha Y, Deng C, Liu B (2008) Development of C-18-functionalized magnetic silica nanoparticles as sample preparation technique for the determination of ergosterol in cigarettes by microwave-assisted derivatization and gas chromatography/mass spectrometry. *J Chromatogr A* 1198:27–33. doi:10.1016/j.chroma.2008.05.049
- Aguilar-Arteaga K, Rodriguez JA, Barrado E (2010) Magnetic solids in analytical chemistry: a review. *Anal Chim Acta* 674(2):157–165. doi:10.1016/j.aca.2010.06.043

31. Deng H, Li XL, Peng Q, Wang X, Chen JP, Li YD (2005) Monodisperse magnetic single-crystal ferrite microspheres. *Angew Chem Int Ed* 44(18):2782–2785. doi:10.1002/anie.200462551
32. Smith HL, Waltman P (1995) The theory of the chemostat: dynamics of microbial competition. Cambridge University Press, New York
33. Brady JF (1995) In: Karu A, Nelson J, Wong R (eds) *Immunoanalysis of agrochemicals: emerging technologies*. American Chemical Society, Washington, pp 266–287
34. Meyer A, Megerle JA, Kuttler C, Mueller J, Aguilar C, Eberl L, Hense BA, Raedler JO (2012) Dynamics of AHL mediated quorum sensing under flow and non-flow conditions. *Phys Biol* 9(2). doi:10.1088/1478-3975/9/2/026007
35. Adar YY, Simaan M, Ulitzur S (1992) Formation of the LuxR protein in the *Vibrio fischeri* lux system is controlled by HtpR through the GroESL proteins. *J Bacteriol* 174(22):7138–7143
36. Ulitzur S (1989) The regulatory control of the bacterial luminescence system—a new view. *J Biolumin Chemilumin* 4(1):317–325. doi:10.1002/bio.1170040144
37. Rampioni G, Bertani I, Pillai CR, Venturi V, Zennaro E, Leoni L (2012) Functional characterization of the quorum sensing regulator RsaL in the plant-beneficial strain *Pseudomonas putida* WCS358. *Appl Environ Microbiol* 78(3):726–734. doi:10.1128/aem.06442-11
38. Gupta R, Schuster M (2013) Negative regulation of bacterial quorum sensing tunes public goods cooperation. *ISME J* 7(11):2159–2168. doi:10.1038/ismej.2013.109
39. Kuttler C, Hense BA (2010) Finetuning for the mathematical modeling of quorum sensing regulation systems. *Int J Biomath Biostat* 1: 151–168
40. Zhang H-B, Wang L-H, Zhang L-H (2002) Genetic control of quorum-sensing signal turnover in *Agrobacterium tumefaciens*. *Proc Natl Acad Sci* 99(7):4638–4643. doi:10.1073/pnas.022056699
41. Chen CC, Riadi L, Suh SJ, Ohman DE, Ju LK (2005) Degradation and synthesis kinetics of quorum-sensing autoinducer in *Pseudomonas aeruginosa* cultivation. *J Biotechnol* 117(1):1–10. doi:10.1016/j.jbiotec.2005.01.003
42. Henkel M, Schmidberger A, Kuehnert C, Beuker J, Bernard T, Schwartz T, Syldatk C, Hausmann R (2013) Kinetic modeling of the time course of N-butyryl-homoserine lactone concentration during batch cultivations of *Pseudomonas aeruginosa* PAO1. *Appl Microbiol Biotechnol* 97(17):7607–7616. doi:10.1007/s00253-013-5024-5
43. De Kievit TR, Gillis R, Marx S, Brown C, Iglewski BH (2001) Quorum-sensing genes in *Pseudomonas aeruginosa* biofilms: their role and expression patterns. *Appl Environ Microbiol* 67(4):1865–1873. doi:10.1128/aem.67.4.1865-1873.2001
44. Lopez D, Vlamakis H, Kolter R (2009) Generation of multiple cell types in *Bacillus subtilis*. *FEMS Microbiol Rev* 33(1):152–163. doi:10.1111/j.1574-6976.2008.00148.x